An Improvement of Steerable Pyramid Denoising Method

E. Ehsaeyan*(C.A.)

Abstract: The use of wavelets in denoising, seems to be an advantage in representing well the details. However, the edges are not so well preserved. Total variation technique has advantages over simple denoising techniques such as linear smoothing or median filtering, which reduce noise, but at the same time smooth away edges to a greater or lesser degree. In this paper, an efficient denoising method based on Total Variation model (TV), and Dual-Tree Complex Wavelet Transform (DTCWT) is proposed to incorporate both properties. In our method, TV is employed to refine low-passed coefficients and DTCWT is used to shrink high-passed noisy coefficients to achieve more accurate image recovery. The efficiency of our approach is firstly analyzed by comparing the results with well-known methods such as probShrink, BLS-GSM, SUREbivariate, NL-Means and TV model. Secondly, it is compared to some denoising methods, which have been reported recently. Experimental results show that the proposed method outperforms the Steerable pyramid denoising by 8.5% in terms of PSNR and 17.5% in terms of SSIM for standard images. Obtained results convince us that the proposed scheme provides a better performance in noise blocking among reported state-of-the-art methods.

Keywords: Complex Wavelet Transform, Denoising, Dual-Tree, Steerable Pyramid, Total Variation.

1 Introduction

Images are used in almost every discipline of science and engineering. Many of them contain noise that makes the observers' job difficult to study the image objects. There are many reasons behind the presence of noise in most of the images, including the artifacts of the image acquisition devices, e.g., cameras. Hence, image denoising plays an important role in the image and video processing. Removing unknown additive noises from measured corrupted images has received much attention in the past fifty years. A complex wavelet transform based on the steerable structure has been reported [1]. In this paper, a new wavelet-domain structure-driven denoising technique with complex bandpass filters has been introduced. However, the lowpass filter smoothens the image. So, the output was blurred and some details were missed in this method.

A minimum risk shrinkage operator for multi-scale Poisson image denoising has been proposed [2]. The authors employed Skellam distribution to minimize the risk function in the multiscale Poisson image denoising setting.

Iranian Journal of Electrical & Electronic Engineering, 2016.
Paper received 04 August 2015 and accepted 23 January 2016.
* The Author is with the Department of Electrical Engineering, Sirjan University of Technology, Sirjan, Iran.
E-mail: ehsaeyan@sirjantech.ac.ir.

An efficient algorithm for adaptive noise reduction with wavelet packet thresholding function has been presented [3]. In this method, the wavelet packet transform was used along with Optimal Wavelet Basis (OWB) for the image decomposition. Then, for each wavelet subband, an adaptive threshold was considered.

Rabbani and Gazor have employed the complex wavelet transform and unconditional Bessel K-form prior density in order to derive Maximum A-Posteriori (MAP) and minimum mean-squared error (MMSE) estimators for video noise reduction in the 3D space [4].

A research on solving Total Variation (TV) problem based on Bayesian MAP has been introduced [5]. In this work, a combination of Reweighted Least Squares (RLS) algorithm with MAP estimation has been used to approach a filter for TV denoising. An Exponential Total Variation model (ETV) with a fast numerical design algorithm has been proposed [6]. The authors utilized higher-order TV models to overcome undesirable 'block' effects in denoised images.

Wang *et al.* have analyzed TV model and proposed an edge-adaptive guiding function based on standard gradient for remote-sensing images [7]. S-model (The proposed method name) could adjust the smooth intensity around edge and keep texture details perfectly. Afonso and Sanches have employed total variation to reconstruct images or volumes from a partial set of observations [8]. They could achieve a lower

reconstruction error with applying the *Augmented Lagrangian* framework. Another research on Photo-Response Non-Uniformity (PRNU) noise extraction has been done for digital cameras [9]. This method has employed total variation technique and could recover noisy images faster than wavelet-based methods.

Sun *et al.* have introduced a biorthogonal balanced multi-wavelet algorithm with armlets order [10]. In another work, Riesz transform has been employed to construct wavelet templates that are best matched to a particular class of images [31]. They have applied Principal Component Analysis (PCA) to optimize the basis functions for image denoising and feature extraction. However, the introduced algorithm is poor and cannot stop noise properly.

In this paper, we present a new denoising approach based on steerable pyramid decomposition. The main contribution of this paper is to improve the PSNR criterion in this framework utilizing the Total Variation model (TV) and Dual-Tree Complex Wavelet Transform (DTCWT). The proposed approach is compared with some well-known related denoising methods such as probShrink, BLS-GSM, SUREbivariate, NL-Means and TV model.

The remainder of the paper is organized as follows: Section 2 describes the principles of three denoising algorithms briefly. Steerable Pyramid algorithm with decomposition and reconstruction block diagram with relevant formulas is given in part one. Complex dual-tree wavelet transform and its advantages over discrete wavelet transform is reviewed in part two; and in part three, total variation model is explained with minimization energy equation. Experimental results are presented and discussed in Section 4. We compare the performance of the proposed method with several existing approaches in image denoising issue. Finally, in Section 6, a conclusion of the paper is given.

2 Background

Before introducing the proposed scheme, three denoising algorithms, which are related to the introduced framework, are reviewed.

2.1 Steerable Pyramid Algorithm

Wavelet decomposition has a disadvantage of shift-invariant. To overcome this problem, the Steerable Pyramid has been introduced [11]. The Steerable Pyramid is a linear multi-scale, multi-orientation image decomposition that provides a useful front-end for image-processing and computer vision applications. The block diagram of the steerable pyramid algorithm is shown in Fig. 1. First, the image passes through high-pass H_0 and low-pass L_0 filter.

The low-pass subimage is then divided into a set of oriented bandpass subimages using filters $(B_1, B_2, \dots, B_k)$ and a low(er)-pass subimage using filter L_1, where *k* is the number of bandpass filters.

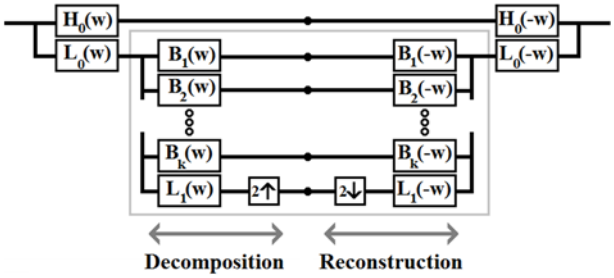

Fig. 1 Decomposition and reconstruction of the steerable pyramid algorithm.

In order to avoid aliasing in the band-pass part, the band-pass components are not downsampled. Therefore, the low(er)-pass subband is sampled by a factor of 2 in the horizontal and vertical directions. The recursive construction of a pyramid is achieved by inserting a copy of the shaded portion of the diagram at the location of the solid circle. The set of filters used in this linear decomposition are highly constrained. First of all, to ensure elimination of the aliasing terms, the filter L_1 should be band-limited, i.e. [11].

$$L_1(\omega) = 0, \ for \ |\omega| > \pi/2 \tag{1}$$

Furthermore, to avoid amplitude distortion, the transfer function of the system should be equal to unity.

$$|H_0(\omega)|^2 + |L_0(\omega)|^2 \left[|L_1(\omega)|^2 + \sum_{i=1}^{k} |B_i(\omega)|^2 \right] = 1 \tag{2}$$

Moreover, in order to cascade the system recursively, another constraint must be verified:

$$|L_1(\omega/2)|^2 = |L_1(\omega)|^2 \left[|L_1(\omega)|^2 + \sum_{i=1}^{k} |B_i(\omega)|^2 \right] \tag{3}$$

The angular constraint on the band-pass filters *BK* is determined by the condition of steerability and can be expressed as:

$$B_k(\omega) = B(\omega)[-jcos(\theta - \theta_k)]^n \tag{4}$$

where for $\theta = \arg(\omega)$, $\theta_k = k\pi/(n+1)$, and

$$B(\omega) = \sqrt{\sum_{i=1}^{K} B_k(\omega)} \tag{5}$$

2.2 Complex Dual Tree Wavelet

The wavelet transform and its family have been considered recently in the signal and image denoising issue [14]. An edge preserving image denoising technique and a filter bank framework, which integrates wavelet filter bank and diamond quincunx filter bank, has been reported [13].

Similar to the discrete wavelet transform, the Dual-Tree Complex Wavelet Transform (DT-CWT) is a multiresolution transform with decimated subbands providing perfect reconstruction of the input [16]. DT-CWT is an enhancement to the Discrete Wavelet Transform (DWT), with important wavelet properties.

In contrast, it uses analytic filters instead of real ones and thus overcomes problems of the DWT at the expense of moderate redundancy.

The DT-CWT is implemented using two real DWTs; DT-CWT can be informed by the existing theory and practice of real wavelet transforms. The DT-CWT gives much better directional selectivity when filtering multi-dimensional signals, and there is an approximate shift invariance. The 2D Dual Tree Complex Wavelet Transform can be implemented using two distinct sets of separable 2D Wavelet bases, as shown below [16]:

$$\begin{aligned}
&\psi_{1,1}(x,y)=\phi_h(x)\psi_h(y),\ \ \psi_{2,1}(x,y)=\phi_g(x)\psi_g(y)\\
&\psi_{1,2}(x,y)=\phi_h(y)\psi_h(x),\ \ \psi_{2,2}(x,y)=\phi_g(y)\psi_g(x)\\
&\psi_{1,3}(x,y)=\psi_h(x)\psi_h(y),\ \ \psi_{2,3}(x,y)=\psi_g(x)\psi_g(y)\\
&\psi_{3,1}(x,y)=\phi_g(x)\psi_h(y),\ \ \psi_{4,1}(x,y)=\phi_h(x)\psi_g(y)\\
&\psi_{3,2}(x,y)=\phi_h(y)\psi_g(x),\ \ \psi_{4,2}(x,y)=\phi_g(y)\psi_h(x)\\
&\psi_{3,3}(x,y)=\psi_h(x)\psi_h(y),\ \ \psi_{4,3}(x,y)=\psi_h(x)\psi_g(y)
\end{aligned} \tag{6}$$

The relationship between wavelet filters h and g is shown below

$$g_0(n)\approx\begin{cases}h_0(n-1) & for\ j=1\\ h_0(n-0.5) & for\ j>1\end{cases} \tag{7}$$

where j is the decomposition level.

2.3 Total Variation

Total variation denoising model has been proposed by Rudin, Osher, and Fatemi (ROF) [17]. The idea behind the model is to exhibit the reconstructed image as the minimizer of an energy functional

$$u=\arg min_{u\in BV(\Omega)}\{|u|_{BV}+\lambda||u-f||_{L^2}^2\} \tag{8}$$

for a suitable parameter $\lambda>0$. Here Ω is a domain in R^N with Lipschitz boundary modeling the image region, e.g. a computer screen. The function f represents the observed and possibly noisy image, which is an element of $L^2(\Omega)$. The regularization functional is the BV-seminorm, defined via

$$|u|_{BV}=\sup_{|g|_\infty\le 1,\,g\in C_c^1(\Omega)^2}\int u(\nabla.g)dx \tag{9}$$

where $|g|=\sqrt{g_1^2+g_2^2}$ and $C_c^1(\Omega)$ denotes the class of continuously differentiable functions of compact support in Ω .The key feature of total variation regularization is the fact that it allows for (and even favours) discontinuous solutions, i.e., images with sharp edges.

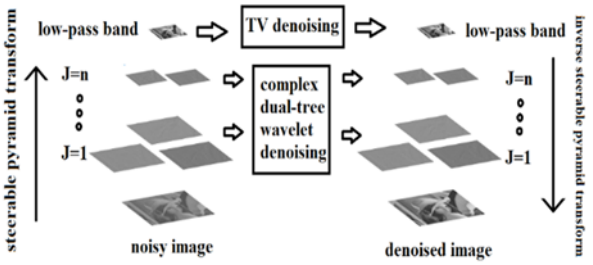

Fig. 2 Proposed denoising algorithm.

Nevertheless, this regularization suppresses oscillations and can still eliminate high-frequency noise.

3 The Proposed Algorithm

Fig. 2 illustrates the proposed denoising scheme. In this framework, complex dual-tree wavelet transform is employed, because wavelets are able to denoise the particular signals and images far better than conventional filters that are based on Fourier transform design, and that do not follow the algebraic rules obeyed by the wavelets. Total variation denoising is used for the low-pass band because of its advantage over linear smoothing or median filtering, which reduces noise but at the same time smooths away edges to a greater or lesser degree. By contrast, total variation denoising is remarkably effective at simultaneously preserving edges whilst smoothing away noise in flat regions, even at low signal-to-noise ratios [18]. The process is as follows: At first, a steerable pyramid transform is applied to the noisy image to decompose it into low and high bands. The high-pass bands are refined by employing DTCWT in different levels and the low-pass band is denoised in the total variation method. Finally, a denoised image is achieved by applying inverse steerable pyramid transform. Table 1 shows the approach in details.

We will show in next section that this structure improves noise eliminating compared to traditional steerable pyramid denoising.

Table 1 Algorithm for proposed denoising method

1- Apply the *n*-level steerable filter decomposition to the noisy image, yielding a set of bandpass channels $\boldsymbol{f_s^{(l)}(m,n,\phi_s)}$. (steered output in direction $\boldsymbol{\phi_s}$ at level $\boldsymbol{l}$)

2- Start TV denoising and reconstruction process at the coarsest scale by setting $\boldsymbol{l=L}$. With $\boldsymbol{\lambda_{max}=0.4}$ and max irritation=300

3- For level j=1 to j=L-1

3-a Apply DTCWT to each directional bands$\boldsymbol{f_s^{(l)}(m,n,\phi_s)}$ to produce different frequency subbands labeled $\boldsymbol{L^k, H^k, D^k, V^k}$, where k=1,…,JJ

3-b- Leave lowpass band $\boldsymbol{L^k}$ unchanged

3-c Calculate the local noise variance $\boldsymbol{\sigma_{noise}^2}$ as [15]

$$\boldsymbol{\sigma_{noise}^2=\frac{median(D^k)}{0.6745}}$$

For each subband $\boldsymbol{H^k, D^k, V^k}$ apply NeighShrink to estimate unknown noiseless coefficient as [12]

3-c-1 For each noisy wavelet coefficient $\boldsymbol{w_{ij}}$ to be shrinked, it incorporates a square neighbouring window $\boldsymbol{B_{ij}}$centered at it. The window size can be 3×3 or 5×5.

3-c-2 Calculate summation $\boldsymbol{S_{ij}^2=\sum_{m,n\in B_{ij}}w_{mn}^2}$

3-c-3 Modify the noisy coefficient by

$$\boldsymbol{\hat{w}_{ij}=w_{ij}\eta_{ij}}\ \text{where}\ \boldsymbol{\eta_{ij}=\max(1-\frac{\sigma_{noise}^2}{S_{ij}^2},0)}$$

3-d Obtain the reconstructed subband $\boldsymbol{H^k, D^k, V^k}$ after applying NeighShrink rule.

3-e Generate a reconstructed version of the image at level j.

4- Apply inverse Steerable Pyramid transform to modified directional subbands $\boldsymbol{f_s^{(l)}(m,n,\phi_s)}$ to obtain refined image.

4 Results and Discussion

There are some failures in the previous research. In Ref. [1], a complex wavelet transform has been used to decompose the noisy image and isotropic lowpass filter to refine the image in a manner appropriate to the local structure. We have not used lowpass filter in our scheme. Hence, the edges and details are preserved better than Ref. [1]. Fig. 3 shows this difference between our and Ref. [1] algorithm.

a- Noisy image (PSNR=18.57 dB)

b- Ref. [1] (PSNR=27.24 dB)

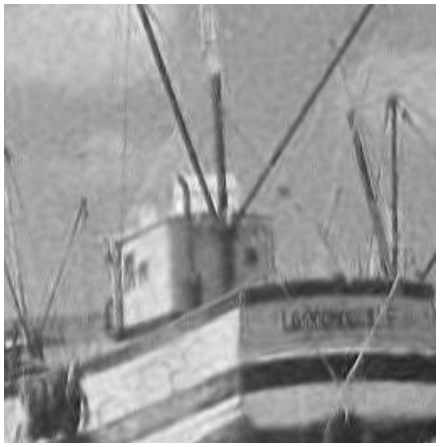

c- Our algorithm (PSNR=27.58 dB)

Fig. 3 Denoising of "boat" image by Ref. [1] and our algorithm. It is obvious that our scheme gives more details in the output denoised image.

In conventional steerable pyramid denoising, a thresholding rule such as 'soft', 'semisoft', 'hard' [19] or 'block' [20] is used to shrink the noisy coefficients. The hard thresholding is defined as

$$y = \begin{cases} x & if \quad |x| > T \\ 0 & if \quad |x| \le T \end{cases} \tag{10}$$

Where x and y are noisy and denoised coefficients and threshold level T is applied. This thresholding performs a binary decision that might introduces artifacts. A less aggressive nonlinearity is the soft thresholding

$$y = \max\left(1 - \frac{T}{|x|}\right) x \tag{11}$$

In our method, the 'block' shrinkage is applied to DTCWT coefficients and low-pass band is refined by TV denoising.

We have found that the number of decomposition level in Steerable Pyramid transform and Dual-Tree Complex Wavelet Transform (DTCWT) of input image affects on output quality. Fig. 4 shows the results of different Steerable Pyramid decomposition levels versus DTCWT levels for "cameraman" image.

It is clear that increasing decomposition level does not improve PSNR. However, it increases computational cost in the algorithm. According to this figure, we have chosen 3 levels for Steerable Pyramid transform decomposition and 3 levels for Dual-Tree Complex Wavelet Transform decomposition empirically.

Two famous criteria, PSNR and SSIM [21], are used to evaluate the performance of the proposed framework. PSNR and SSIM have been calculated for standard images with the size of 512×512 pixels in various noise levels. The images are corrupted with Additive White Gaussian Noise (AWGN). Table 2 compares PSNRs and SSIMs of traditional steerable pyramid and proposed method. It is clear that our scheme improves these criteria efficiently.

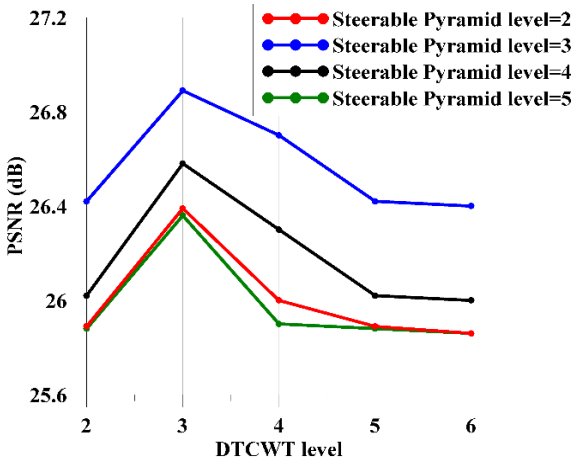

Fig. 4 The effect of Steerable Pyramid decomposition levels and DTCWT levels on output PSNR for "cameraman" image ($\sigma = 30$).

Table 2 Comparative PSNR and SSIM values with different noises for traditional Steerable pyramid denoising and our method.

		PSNR			SSIM		
512×512 image	sigma	Noisy image	Steerable pyramid denoising [11]	Proposed method	Noisy image	Steerable pyramid denoising [11]	Proposed method
Lena	20	22.11	29.38	31.68	0.42	0.77	0.87
	30	18.59	27.69	29.79	0.32	0.68	0.81
	40	16.09	26.31	28.43	0.26	0.60	0.75
	50	14.15	25.08	27.39	0.23	0.54	0.70
	60	12.57	23.95	26.73	0.20	0.49	0.69
Barbara	20	22.11	29.49	30.08	0.60	0.54	0.54
	30	18.59	28.12	29.60	0.56	0.52	0.52
	40	16.09	26.73	28.93	0.54	0.51	0.51
	50	14.15	25.42	28.32	0.52	0.51	0.51
	60	12.57	24.22	27.91	0.51	0.50	0.51
Peppers	20	22.11	27.67	30.84	0.43	0.73	0.81
	30	18.59	26.46	29.08	0.32	0.65	0.76
	40	16.09	25.38	27.59	0.26	0.59	0.71
	50	14.15	24.37	26.55	0.22	0.53	0.68
	60	12.57	23.39	25.92	0.19	0.49	0.66
Boat	20	22.11	26.59	29.23	0.49	0.67	0.76
	30	18.59	25.65	27.59	0.38	0.61	0.70
	40	16.09	24.76	26.30	0.30	0.55	0.66
	50	14.15	23.87	25.36	0.26	0.50	0.62
	60	12.57	23.00	24.76	0.23	0.45	0.60
Couple	20	22.11	26.21	28.91	0.51	0.67	0.78
	30	18.59	25.29	27.04	0.39	0.61	0.71
	40	16.09	24.47	25.87	0.32	0.56	0.66
	50	14.15	23.63	25.04	0.27	0.51	0.61
	60	12.57	22.79	24.48	0.23	0.47	0.58

Fig. 5 illustrates comparative results of the traditional steerable denoising and proposed framework for the image ‘Couple’. According to the obtained results, it is obvious that our method yields a better quality. We have implemented Ref. [11] denoising method in Pentium 5 vs core 2 duo computer and compared the time execution in method [11] with our method. The average time estimated in method [11] is 0.92 seconds and in our method is 8.7 seconds.

Table 3 compares the ability of noise blocking of introduced scheme with that of well-known denoising methods. The best PSNR is bold in every column.

a- Noisy image (sigma=30)

b- Steerable Pyramid denoising [11]

c- Proposed method

Fig. 5 Visual results of Steerable pyramid denoising and proposed method for cropped image ‘couple’.

The results convince us that our method has higher PSNRs in most noise levels.

Another comparison is given in Table 4, where results of the introduced framework are compared to recent reported denoising methods for images ‘Lena’, ‘Barbara’ and ‘Peppers’. Similar to previous tables, this

table also confirms the superiority of our framework over recent reported methods.

Table 3 The compared results of the denoising images in different methods.

σ	20	30	40	50	60
Input PSNR	22.11	18.59	16.09	14.15	12.57
Test image	Lena (512 × 512)				
ProbShrink [22]	31.24	29.36	28.01	27.01	26.52
BLS-GSM [23]	31.32	29.47	28.21	27.19	26.71
SUREbivariate [24]	31.37	29.56	28.31	27.37	26.77
NL-means [32]	31.16	28.3	26.98	25.8	24.46
TV model [17]	30.6	28.87	27.56	26.58	25.63
Our method	31.68	29.79	28.43	27.39	26.73
Test image	Barbara (512 × 512)				
ProbShrink [22]	28.4	26.27	24.89	23.86	23.32
BLS-GSM [23]	28.28	25.92	24.44	23.5	22.87
SUREbivariate [24]	27.98	25.83	24.54	23.7	23.15
NL-means [32]	27.42	24.16	23.69	22.57	21.89
TV model [17]	26.32	24.73	23.85	23.17	22.79
Our method	30.08	29.6	28.93	28.32	27.91
Test image	Cameraman (256 × 256)				
ProbShrink [22]	28.25	26.13	24.78	23.8	22.83
BLS-GSM [23]	28.29	26.24	24.94	24.03	23
SUREbivariate [24]	28.51	26.48	25.11	24.1	23.29
NL-means [32]	27.59	25.23	23.44	22.28	21.51
TV model [17]	27.91	26.12	24.98	24.02	23.1
Our method	28.20	26.58	25.27	24.18	23.38

Table 4 PSNR performance data of proposed scheme and recent state-of-the-art works.

	LENA		**BARBARA**		**PEPPERS**	
σ	20	30	20	30	20	30
[25]	30.77	29.04	28.55	27.38	30.57	28.83
[26]	30.92	29.13	28.48	26.27	30.57	28.83
[27]	28.25	25.7	26.81	24.49	26.96	25.03
[28]	31.16	29.25	28.71	26.59	30.81	28.92
[29]	30.61	28.73	26.57	26.36	29.31	27.85
[30]	30.42	28.54	26.28	24.73	30.17	28.28
OUR WORK	31.68	29.79	30.08	29.60	30.84	29.08

5 Conclusion

In this paper, we presented a new steerable pyramid denoising method based on dual-tree complex wavelet transform (DTCWT) and total variation model that effectively produce denoised image with minimum artifacts. The significant purpose of the paper is to improve Peak Signal to Noise Ratio (PSNR) in steerable pyramid structure. We showed that the proposed structure improves steerable pyramid denoising criteria. In different noise level, the results demonstrated significant improvement over traditional steerable pyramid theory. Experiments were conducted on different test standard images, which were corrupted by various noise levels, to assess the performance of the proposed algorithm. The obtained results revealed the superiority of our scheme compared to some of the best state-of-the-art methods. In future, we plan to extend the introduced scheme to other wavelet families such as double-density dual-tree complex wavelet transform for further improvement in the performance.

References

[1] A. Bharath and J. Ng, "A steerable complex wavelet construction and its application to image denoising", *IEEE Transactions on Image Processing*, Vol. 14, No. 7, pp. 948–959, 2005.

[2] W. Cheng and K. Hirakawa, "Minimum Risk Wavelet Shrinkage Operator for Poisson Image Denoising", *IEEE Transactions on Image Processing*, Vol. 24, No. 5, pp. 1660-1671, 2015.

[3] A. Fathi and A. R. Naghsh-Nilchi, "Efficient Image Denoising Method Based on a New Adaptive Wavelet Packet Thresholding Function", *IEEE Transactions on Image Processing*, Vol. 21, No. 9, pp. 3981–3990, 2012.

[4] H. Rabbani and S. Gazor, "Video denoising in three-dimensional complex wavelet domain using a doubly stochastic modelling", *IET Image Processing*, Vol. 6, No. 9, pp. 1262–1274, 2012.

[5] M. V. Afonso and J. M. Sanches, "A total variation recursive space-variant filter for image denoising", *Digital Signal Processing*, Vol. 40, No. C, pp. 101–116, 2015.

[6] C. Sun, C. Tang, X. Zhu and H. Ren, "Exponential total variation model for noise removal, its numerical algorithms and applications", *AEU - International Journal of Electronics and Communications*, Vol. 69, No. 3, pp. 644–654, 2015.

[7] X. Wang, Y. Liu, H. Zhang and L. Fang, "A total variation model based on edge adaptive guiding function for remote sensing image de-noising", *International Journal of Applied Earth Observation and Geoinformation*, Vol. 34, pp. 89–95, 2015.

[8] M. Afonso and J. M. Sanches, "Image reconstruction under multiplicative speckle noise

using total variation", *Neurocomputing*, Vol. 150, No. A, pp. 200–213, 2015.
[9] F. Gisolf, A. Malgoezar, T. Baar and Z. Geradts, "Improving source camera identification using a simplified total variation based noise removal algorithm", *Digital Investigation*, Vol. 10, No. 3, pp. 207–214, 2015.
[10] J. Sun, W. Wang, L. Zhao and L. Cui, "Biorthogonal balanced multiwavelets with high armlets order and their application in image denoising", *Mathematics and Computers in Simulation*, Vol. 111, pp. 48–62, 2015.
[11] E. Simoncelli and W. Freeman, "The steerable pyramid: a flexible architecture for multi-scale derivative computation", *Proc. Int. Conf. on Image Processing*, Vol. 3, pp. 444–447, 1995.
[12] T. Cai, B.W. Silverman, "Incorporating information on neighboring coefficients into wavelet estimation", *Sankhya, Ser. B*, Vol. 63, No. 2, pp. 127–148, 2001.
[13] S. A. Shanthi, C. H. Sulochana, and T. Latha, "Image denoising in hybrid wavelet and quincunx diamond filter bank domain based on Gaussian scale mixture model", *Computers & Electrical Engineering*, Vol. 46, pp. 384-393, August 2015.
[14] W. Zhang, J. Li and Y. Yang, "Spatial fractional telegraph equation for image structure preserving denoising", *Signal Processing*, Vol. 107, pp. 368-377, February 2015.
[15] D. Donoho, "De-noising by soft-thresholding", *IEEE Trans. on Information Theory*, Vol. 41, No. 3, pp. 613–627, 1995.
[16] I. Selesnick, R. Baraniuk and N. Kingsbury, "The dual-tree complex wavelet transform", *IEEE Signal Process. Mag*, Vol. 22, No. 6, pp. 123–151, 2005.
[17] L. I. Rudin, S. Osher and E. Fatemi, "Nonlinear total variation based noise removal algorithms", *Physica D: Nonlinear Phenomena*, Vol. 60, No. 1-4, pp. 259–268, 1992.
[18] D. Strong and T. Chan, "Edge-preserving and scale-dependent properties of total variation regularization", *Inverse Problems*, Vol. 19, No. 6, pp. 165-187, 2003.
[19] A. Bruce, H. Gao, "Wave shrinkage: functions and threshold", *SPIE*, pp. 270–281, 1995.
[20] T. Cai, B. Silverman, "Incorporating information on neighboring coefficients into wavelet estimation", *The Indian Journal of Statistics*, Vol. 63, No. B, pp. 127-148, 2001.
[21] Z. Wang, A. Bovik, H. Sheikh and E. Simoncelli, "Image Quality Assessment: From Error Visibility to Structural Similarity", *IEEE Trans. on Image Process.*, Vol. 13, No. 4, pp. 600-612, 2004.
[22] A. Pizurica and W. Philips, "Estimating the probability of the presence of a signal of interest in multiresolution single- and multiband image denoising", *IEEE Trans. on Image Process.*, Vol. 15, No. 3, pp. 654–665, 2006.
[23] J. Portilla, V. Strela, M. Wainwright and E. Simoncelli, "Image denoising using scale mixtures of gaussians in the wavelet domain", *IEEE Trans. on Image Process.*, Vol. 12, No. 11, pp. 1338–1351, 2003.
[24] F. Luisier, T. Blu and M. Unser, "A New SURE Approach to Image Denoising: Interscale Orthonormal Wavelet Thresholding", *IEEE Trans. on Image Process.*, Vol. 16, No. 3, pp. 593–606, 2007.
[25] H. Om and M. Biswas, "A generalized image denoising method using neighbouring wavelet coefficients", *Signal, Image and Video Processing SIViP*, Vol. 9, No. 1, pp. 191–200, 2013.
[26] H. Om and M. Biswas, "MMSE based map estimation for image denoising", *Optics & Laser Technology*, Vol. 57, pp. 252–264, 2014.
[27] P. Jain and V. Tyagi, "An adaptive edge-preserving image denoising technique using tetrolet transforms", *The Visual Computer Vis Comput*, Vol. 31, No. 5, pp. 657–674, 2014.
[28] M. Biswas and H. Om, "A New Adaptive Image Denoising Method Based on Neighboring Coefficients", *Journal of The Institution of Engineers* (India): Series B J. Inst. Eng. India Ser. B, 2014.
[29] D. Tian, D. Xue and D. Wang, "A fractional-order adaptive regularization primal–dual algorithm for image denoising", *Information Sciences*, Vol. 296, pp. 147–159, 2015.
[30] N. He, J.-B. Wang, L.-L. Zhang and K. Lu, "An improved fractional-order differentiation model for image denoising", *Signal Processing*, Vol. 112, pp. 180–188, July 2015.
[31] M. Unser, N. Chenouard and D. V. D. Ville, "Steerable Pyramids and Tight Wavelet Frames in $L_2(R^d)$", *IEEE Transactions on Image Processing*, Vol. 20, No. 10, pp. 2705–2721, 2011.
[32] A. Buades, B. Coll and J. M. Morel, "A Review of Image Denoising Algorithms, with a New One", *Multiscale Modeling & Simulation Multiscale Model*, Vol. 4, No. 2, pp. 490–530, 2005.

Ehsan Ehsaeyan received the B.Sc. degree in electronic engineering from Shahed University, Tehran, Iran in 2006 and the M.Sc. Eng degree in communication engineering at University of Shahid Bahonar, Kerman, Iran in 2009. His research interest is image and video processing.